



HAL
open science

Finite Groups for the Kummer Surface: the Genetic Code and a Quantum Gravity Analogy

Michel Planat, David Chester, Raymond Aschheim, Marcelo M Amaral, Fang Fang, Klee Irwin

► To cite this version:

Michel Planat, David Chester, Raymond Aschheim, Marcelo M Amaral, Fang Fang, et al.. Finite Groups for the Kummer Surface: the Genetic Code and a Quantum Gravity Analogy. Quantum Reports, 2021, 3 (1), pp.68-79. 10.3390/quantum3010005 . hal-03100697

HAL Id: hal-03100697

<https://hal.science/hal-03100697>


Submitted on 6 Jan 2021

HAL is a multi-disciplinary open access archive for the deposit and dissemination of scientific research documents, whether they are published or not. The documents may come from teaching and research institutions in France or abroad, or from public or private research centers.


L'archive ouverte pluridisciplinaire **HAL**, est destinée au dépôt et à la diffusion de documents scientifiques de niveau recherche, publiés ou non, émanant des établissements d'enseignement et de recherche français ou étrangers, des laboratoires publics ou privés.

Article

Finite groups for the Kummer surface: the genetic code and a quantum gravity analogy

Michel Planat ¹  0000-0001-5739-546X, David Chester ², Raymond Aschheim

³  0000-0001-6953-8202, Marcelo M. Amaral ⁴  0000-0002-0637-1916, Fang Fang ⁵ and Klee Irwin

⁶  0000-0003-2938-3941

¹ Université de Bourgogne/Franche-Comté, Institut FEMTO-ST CNRS UMR 6174, 15 B Avenue des Montboucons, F-25044 Besançon, France.; michel.planat@femto-st.fr

² Quantum Gravity Research, Los Angeles, CA 90290, USA; DavidC@QuantumGravityResearch.org

³ Quantum Gravity Research, Los Angeles, CA 90290, USA; raymond@QuantumGravityResearch.org

⁴ Quantum Gravity Research, Los Angeles, CA 90290, USA; Marcelo@quantumgravityresearch.org

⁵ Quantum Gravity Research, Los Angeles, CA 90290, USA; fang@quantumgravityresearch.org

⁶ Quantum Gravity Research, Los Angeles, CA 90290, USA; Klee@quantumgravityresearch.org

* Correspondence: michel.planat@femto-st.fr

Version January 6, 2021 submitted to Journal Not Specified

Abstract: The Kummer surface was constructed in 1864. It corresponds to the desingularisation of the quotient of a 4-torus by 16 complex double points. Kummer surface is known to play a role in some models of quantum gravity. Following our recent model of the DNA genetic code based on the irreducible characters of the finite group $G_5 := (240, 105) \cong \mathbb{Z}_5 \rtimes 2O$ (with $2O$ the binary octahedral group), we now find that groups $G_6 := (288, 69) \cong \mathbb{Z}_6 \rtimes 2O$ and $G_7 := (336, 118) \cong \mathbb{Z}_7 \rtimes 2O$ can be used as models of the symmetries in hexamer and heptamer proteins playing a vital role for some biological functions. Groups G_6 and G_7 are found to involve the Kummer surface in the structure of their character table. An analogy between quantum gravity and DNA/RNA packings is suggested.

Keywords: Kummer surface, DNA genetic code, hexamers and pentamers, informationally complete characters, finite groups, hyperelliptic curve

PACS: 02. 20.-a, 02.10.-v, 03.65.Fd, 82.39.Rt, 87.10.-e, 87.14.gk

1. Introduction

In a recent paper we found that the 22 irreducible characters of the group $G_5 := (240, 105) \cong \mathbb{Z}_5 \rtimes 2O$, with $2O$ the binary octahedral group, could be made in one-to-one correspondence with the DNA multiplets encoding the proteinogenic amino acids [1]. The cyclic group \mathbb{Z}_5 features the five-fold symmetry of the constituent bases, see Fig. 1a. An important aspect of this approach is that the irreducible characters of G_5 may be seen as ‘magic’ quantum states carrying minimal and complete quantum information, see [1]–[3] for the meaning of these concepts. It was also shown that the physical structure of DNA was reflected in some of the entries of the character table including the Golden ratio, the irrational number $\sqrt{2}$, as well as the four roots of a quartic polynomial.

In molecular biology, there exists an ubiquitous family of RNA-binding proteins called LSM proteins whose function is to serve as scaffolds for RNA oligonucleotides, assisting the RNA to maintain the proper three-dimensional structure. Such proteins organize as rings of six or seven subunits. The Hfq protein complex was discovered in 1968 as an Escherichia coli host factor that was essential for replication of the bacteriophage $\phi\beta$ [4], it displays an hexameric ring shape shown in Fig. 1b.

27 It is known that, in the process of transcription of DNA to proteins through messenger RNA
 28 sequences (mRNAs), there is an important step performed in the spliceosome [5]. It consists of
 29 removing the non-coding intron sequences for obtaining the exons that code for the proteinogenic
 30 amino acids. A ribonucleoprotein (RNP) –a complex of ribonucleic acid and RNA-binding protein–
 31 plays a vital role in a number of biological functions that include transcription, translation, the
 32 regulation of gene expression and the metabolism of RNA. Individual LSm proteins assemble into
 33 a six or seven member doughnut ring which usually binds to a small RNA molecule to form a
 34 ribonucleoprotein complex.

35 Thus, while fivefold symmetry is inherent to the bases *A, T, G, C* –the building blocks of DNA–,
 36 six-fold and seven-fold symmetries turn out to be the rule at the level of the spliceosome [6]. Of the five
 37 small ribonucleoproteins, four of them called U1, U2, U4 and U5, contain an heptamer ring, whereas
 38 the U6 contains a specific Lsm2-8 heptamer with seven-fold symmetry. A specific Lsm heptameric
 39 complex Lsm1-7 playing a role in mRNA decapping is shown in Fig. 1c [7].

40 Observe that six-fold rings are also present in other biological functions such as genomic DNA
 41 replication [8,9]. The minichromosome maintenance complex (MCM) hexameric complex (Mcm2–7)
 42 forms the core of the eukaryotic replicative helicase. Eukaryotic MCM consists of six gene products,
 43 Mcm2–7, which form a heterohexamer [9]. Deregulation of MCM function has been linked to genomic
 44 instability and a variety of carcinomas.

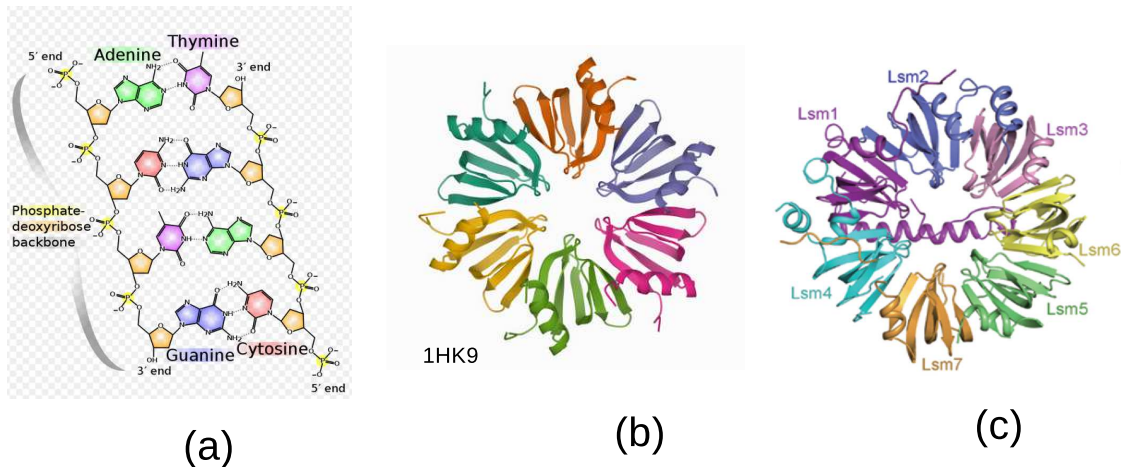


Figure 1. (a) Five-fold symmetry in the DNA, (b) six-fold symmetry in the LSM protein complex Hfq [4], (c) seven-fold symmetry of the Lsm1-7 complex in the spliceosome [7].

45 In this paper, in order to approach these biological issues –the hexamer and pentamer rings–, we
 46 generalize our previous model of the DNA/RNA, which has been based on the five-fold symmetry
 47 group G_5 , to models of DNA/RNA complexes, based on the six-fold symmetry group $G_6 := (288, 69) \cong$
 48 $\mathbb{Z}_6 \times 2O$ and the seven-fold symmetry group $G_7 := (336, 118) \cong \mathbb{Z}_7 \times 2O$.

49 What corresponds to the quartic curve, derived from some of the entries in the character table
 50 of G_5 , is a genus 2 hyperelliptic curve derived from the character table of G_6 or G_7 , underlying the
 51 so-called Kummer surface, a gem of algebraic geometry [11]. The Kummer surface is a prototypic
 52 example of a K_3 surface – a Calabi-Yau manifold of complex dimension two– and as such it is part of
 53 models in string theory and/or quantum gravity.

54 Sec. 2.1 is a brief introduction to elliptic and hyperelliptic curves defined over any field. In Sec.
 55 2.2 and 2.3, the main objective is to describe a construction of the Kummer surface \mathcal{K} based on the
 56 character table of the groups G_6 or G_7 . One identifies the 16 double points of \mathcal{K} as the 16 two-torsion
 57 points of a genus two hyperelliptic curve \mathcal{C} and one provides an explicit description of the group law
 58 and of the Kummer surface.

In Sec. 3, a new encoding of the proteinogenic amino acids by the irreducible characters and the corresponding representations of the group G_7 is described. It improves the description obtained in [1] from the 22 irreducible characters of group G_5 .

In Sec. 4, we browse over some applications of the Kummer surface to models of quantum gravity.

2. The hyperelliptic curve and the attached Kummer surface from groups G_6 and G_7

Let us first recall an important aspect of our previous work. Let G be a finite group with d conjugacy classes. An irreducible character $\kappa = \kappa_r$ corresponding to a r -dimensional representation of G carries quantum information [1]-[3]. It may be calculated thanks to the action of elements of a d -dimensional Pauli group \mathcal{P}_d acting on κ . In other words, the character κ may be seen as the ‘magic state’ of a quantum computation [2,10].

In a concrete way, one defines d^2 one-dimensional projectors $\Pi_i = |\psi_i\rangle\langle\psi_i|$, where the $|\psi_i\rangle$ are the d^2 states obtained from the action of \mathcal{P}_d on κ , and one calculates the rank of the Gram matrix \mathcal{G} with elements $\text{tr}(\Pi_i\Pi_j)$. A Gram matrix \mathcal{G} with rank equal to d^2 is the signature of a minimal informationally complete quantum measurement (or MIC), see e.g. [1, Sec. 3] for more details.

As in our previous work, in a character table, we will display the measure of quantum information of a character $\kappa_r = \kappa$ as the rank of the attached Gram matrix \mathcal{G} .

2.1. Excerpts about elliptic and hyperelliptic curves

Let us consider a curve \mathcal{C} defined with the algebraic equation $y^2 + h(x)y = f(x)$ where $h(x)$ and $f(x)$ are finite degree polynomials with elements in a field K .

For an elliptic curve –let us use the notation \mathcal{E} instead of \mathcal{C} for this case–, polynomials $h(x)$ and $f(x)$ are of degrees 1 and 2, respectively and the genus of \mathcal{E} is $g = 1$. In the Weierstrass form of an elliptic curve, one takes $h(x) = a_1x + a_3$ and $f(x) = x^3 + a_2x^2 + a_4x + a_6$ so that \mathcal{E} is specified with the sequence $[a_1, a_2, a_3, a_4, a_6]$ of elements of K . There is a rich literature about elliptic curves defined over rational fields \mathbb{Q} , complex fields \mathbb{C} , number fields or general fields. Explicit results are documented in tables such as the Cremona table [12] or can be obtained from a mathematical software such as Magma [13].

An elliptic curve (as well as a hyperelliptic curve) may be viewed as embedded in a weighted projective space, with weights 1, $g + 1$ and 1, in which the points at infinity are non singular. In the present work, one meets genus 2 curves for which there exists a set of 16 double points leading to the construction of a Kummer surface. All curves of genus 2 are hyperelliptic but generic curves of genus $g > 2$ are not. Again references [12] and [13] are basic references for explicit results.

There are plenty known invariants of a (hyper)elliptic curve \mathcal{C} over a field. One of them is the conductor N of an elliptic curve \mathcal{E} seen as an abelian variety A . For A defined over \mathbb{Q} , the conductor is the positive integer whose prime factors are the primes where A has a bad reduction. The conductor characterizes the isogeny class of A so that the curves \mathcal{E} over \mathbb{Q} may be classified according to the isogeny classes. Another important invariant is the Mordell-Weil group of A which is the group $A(\mathbb{Q})$ of \mathbb{Q} -rational points of \mathcal{E} . Weil proved that $A(\mathbb{Q})$ is finitely generated with a unique decomposition of the form $A(\mathbb{Q}) \cong \mathbb{Z}^{r_A} \oplus T$, where the finite group T is the torsion subgroup and r_A is the rank of A . This result was later generalized to the elliptic curves defined over any field K . For a hyperelliptic curve, the invariant in the Weierstrass equation of \mathcal{C} called the discriminant Δ may be defined over any field K . For an elliptic curve, this leads to the j -invariant $j = c_4^3/\Delta$ with c_4 a polynomial function of the coefficients in the Weierstrass form.

The main applications of elliptic curves are in the field of public-key cryptography. For hyperelliptic curves, one makes use of the Jacobian as the abelian group in which to do arithmetic, as one uses the group of points on an elliptic curve.

From now we describe how genus 1 curves (elliptic curves) and genus 2 curves (hyperelliptic curves of the Kummer type) arise in the character table of groups of signature $G_i \cong \mathbb{Z}_i \rtimes 2O$, $i = 5, 6$

106 and 7. Other finite groups and curves of genus $g > 2$ built from the character table of a finite group G
 107 are worthwhile to be investigated in the future.

108 Let us illustrate our description with the genus 1 hyperelliptic curve introduced in the context
 109 of our model of the genetic code based on the group $G_5 := (240, 105)$ in which $h(x) = 0$ and
 110 $f(x) = x^4 - x^3 - 4x^2 + 4x + 1$ [1, Sec 5]. Seeing this curve over the rationals, one learns from Magma
 111 [13] that the conductor is $N = 300$ and the discriminant is $\Delta = 18000$. A look at the Cremona table
 112 for elliptic curves [12] allows us to put our curve in the isogeny class of Cremona reference ‘300d1’.
 113 The Weierstass form is $y^2 = x^3 - x^2 - 13x + 22$ and the Mordell-Weil group is the group of infinite
 114 cardinality $\mathbb{Z} \times \mathbb{Z}_2$.

115 Now we use this knowledge to investigate some properties of the character tables of group G_6
 116 and G_7 .

117 2.2. The group $G_6 := (288, 69) \cong \mathbb{Z}_6 \times 2O$

(288,69)	dimension	1	1	1	1	2	2	2	2	2	2
$\mathbb{Z}_6 \times (\mathbb{Z}_2.S_4)$	d-dit, d=30	31	796	867	867	882	882	880	897	897	880
	char	Cte	Cte	I	I	Cte	Cte	z_1	z_2	z_2	z_1
(288,69)	dimension	2	2	2	2	2	2	4	4	4	4
	d-dit, d=30	885	885	885	885	885	885	876	878	899	899
	char	z_3	z_3	z_3	z_3	z_3	z_3	Cte	Cte	I	I
(288,69)	dimension	4	4	4	4	4	4	6	6	6	6
	d-dit, d=30	877	878	885	885	885	885	885	885	880	880
	char	Cte	Cte	z_3	z_3	z_3	z_3	z_3	z_3	Cte	Cte

Table 1. For the group $G_6 := (288, 69) \cong \mathbb{Z}_6 \times 2O$, the table provides the dimension of the representation, the rank of the Gram matrix obtained under the action of the 30-dimensional Pauli group and the entries involved in the characters. All characters are neither faithful nor informationally complete. The notation is $I = \exp(2i\pi/4)$, $z_1 = -\sqrt{2}$, $z_2 = I\sqrt{2}$ and $z_3 = -2 * \cos(\pi/9)$.

118 One first considers the group $G_6 := (288, 69) \cong \mathbb{Z}_6 \times 2O$, with $2O$ the binary octahedral group.
 119 The structure of the character table is shown in Table 1. All characters are neither faithful nor
 120 informationally complete since the rank of the Gram matrix is never $d^2 = 30^2$ for any character.
 121 Some characters contain entries with complex numbers I or $z_2 = I\sqrt{2}$. There are 12 characters
 122 containing entries with $z_3 = -2 * \cos(\pi/9)$ featuring the angle $\pi/9$. We now show an important
 123 characteristics of such characters. As an example, let us write the character number 11 as obtained
 124 from Magma [13]

$$\kappa_{11} = [2, 2, -2, -2, -1, 2, -2, 0, 0, 1, -1, 1, 0, 0, 0, 0, z_3, z_3\#2, z_3\#4, -1, 1, -z_3\#2, -z_3\#4, -z_3\#4, z_3\#2, z_3, -z_3, z_3\#4, -z_3, -z_3\#2]$$

125 where # denotes the algebraic conjugation, that is # k indicates replacing the root of unity w by w^k .
 126 The non constant (but real) entries are $k_{\pm l} = \pm z_3\#l$, with $l = 1, 2$ or 4 . We obtain $k_1 = -2 * \cos(\pi/9)$
 127 and $k_{2,4} = \cos(\pi/9) \mp \cos(2\pi/9) \pm \cos(4\pi/9)$ and $k_1 + k_2 + k_4 = 0$.

128 Following our approach in [1], we construct an hyperelliptic curve C_6 of the form $y^2 = \prod_{\pm l} (x -$
 129 $k_l) = f(x)$. In an explicit way, it is

$$C_6 : y^2 = x^6 - 6x^4 + 9x^2 - 1, \tag{1}$$

130 a genus 2 hyperelliptic curve. Using Magma [13], one gets the polynomial definition of the
 131 Kummer surface $S(x_1, x_2, x_3, x_4)$ as

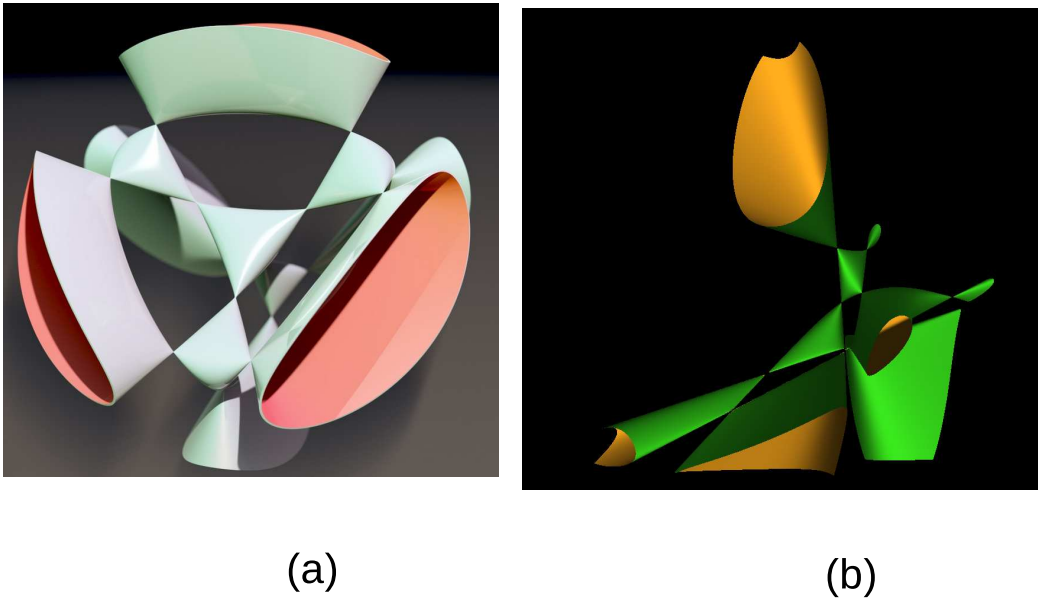


Figure 2. (a) A standard plot of the Kummer surface in its 3-dimensional projection, (b) a section at constant x_4 of the Kummer surface defined in Sec. 2.3.

$$S(x_1, x_2, x_3, x_4) = 36x_1^4 + 4x_1^3x_4 - 24x_1^2x_2^2 + 220x_1^2x_3^2 - 36x_1^2x_3x_4 - 8x_1x_2^2x_3 \\ + 24x_1x_3^2x_4 - 4x_1x_3x_4^2 + 4x_2^4 - 36x_2^2x_3^2 + x_2^2x_4^2 + 24x_3^4 - 4x_3^3x_4.$$

132 The desingularisation of the Kummer surface is obtained in a simple way by restricting the
133 product $f(x) = \prod_{\pm l} (x - k_l)$ to the five first factors with indices $\pm 1, \pm 2$ and 4.

134 One embeds \mathcal{C}_6 in a weighted projective plane, with weights 1, $g + 1$, and 1, respectively on
135 coordinates x, y and z . Therefore, point triples are such that $(x : y : z) = (\mu x : \mu y : \mu z)$, μ in the field of
136 definition, and the points at infinity take the form $(1 : y : 0)$. Below, the software Magma is used for
137 the calculation of points of \mathcal{C}_6 [13]. For the points of \mathcal{C}_6 , there is a parameter called 'bound' that loosely
138 follows the heights of the x -coordinates found by the search algorithm.

139 It is found that the corresponding Jacobian of \mathcal{C}_6 has $16 = 6 + 10$ points as follows

140 * the 6 points bounded by the modulus 1:

141 $Id := (1, 0, 0)$, $K_{\pm 1} := (x - k_{\pm 1}, 0, 1)$, $K_{\pm 2} := (x - k_{\pm 2}, 0, 1)$ and $K_4 = (k_4, 0, 1)$.

142 * the 10 points of modulus > 1 :

143 $a_1 := K_{-1} + K_4$, $a_2 := K_1 + K_{-1}$, $a_3 := K_1 + K_{-2}$, $a_4 := K_1 + K_{-1} + K_2$, $a_5 := K_1 + K_{-1} + K_{-2}$,

144 $a_6 := K_1 + K_4$, $a_7 := K_{-1} + K_2$, $a_8 := K_1 + K_{-1} + K_4$, $a_9 := K_{-1} + K_{-2}$ and $a_{10} := K_1 + K_{-1} + K_2$,

145 The 16 points organize as a commutative group isomorphic to the maximally abelian group \mathbb{Z}_2^4 as
146 shown in the following Jacobian addition table

147 where the blocks are given explicitly as

A	B	C	D
B	A	D	C
C	D	A	B
D	C	B	A

Table 2. The structure of the addition table for the 16 singular Jacobian points of the hyperelliptic curves \mathcal{C}_6 and \mathcal{C}_7 .

$$\begin{aligned}
 A : & \begin{bmatrix} Id & K_1 & K_{-1} & a_2 \\ K_1 & Id & a_2 & K_{-1} \\ K_{-1} & a_2 & Id & K_1 \\ a_2 & K_{-1} & K_1 & Id \end{bmatrix}, & B : & \begin{bmatrix} K_2 & a_{10} & a_7 & a_4 \\ a_{10} & K_2 & a_4 & a_7 \\ a_7 & a_4 & K_2 & a_{10} \\ a_4 & a_7 & a_{10} & K_2 \end{bmatrix}, \\
 C : & \begin{bmatrix} K_{-2} & a_3 & a_9 & a_5 \\ a_3 & K_{-2} & a_5 & a_3 \\ a_9 & a_5 & K_{-2} & a_3 \\ a_5 & a_9 & a_3 & K_{-2} \end{bmatrix}, & D : & \begin{bmatrix} a_8 & a_1 & a_6 & K_4 \\ a_1 & a_8 & K_4 & a_6 \\ a_6 & K_4 & a_8 & a_1 \\ K_4 & a_6 & a_1 & a_8 \end{bmatrix}.
 \end{aligned}$$

148 As a whole, one can check that there are only 48 points in the Jacobian $J(\mathcal{C}_6)$. They
 149 organize at the group $\mathbb{Z}_3 \times \mathbb{Z}_2^3$, i.e. three copies of the group of singular points.

150 2.3. The group $G_7 := (336, 118) \cong \mathbb{Z}_7 \times 2O$

151 Let us consider the group $G_7 := (336, 118) \cong \mathbb{Z}_7 \rtimes 2O$, with $2O$ the binary
 152 octahedral group. The structure of the character table is shown in the table of section
 153 3 about a refined model of the genetic code. Except for the singlets, the irreducible
 154 characters of G_7 are informationally complete (with rank of the Gram matrix equal
 155 to $d^2 = 29^2$ for any character). Only the first two singlets are exceptions. The entries
 156 involved in the characters are $z_1 = 2 \cos(2\pi/7)$, $z_2 = 2z_1$, $z_3 = -6 \cos(\pi/7)$, $z_4 = \sqrt{2}$
 157 and $z_5 = 2 \cos(2\pi/21)$ featuring the angles $2\pi/8$ (in z_4), $2\pi/7$ and $2\pi/21$. There are
 158 9 faithful characters over the 10 quartets.

Character	z_i powers	$f(x)$ polynomial	Cremona ref.
4-6	$z_1 : [1, 2, 3]$	$x^3 + x^2 - 2x - 1$	784 <i>i</i> ₁
18-20	$z_1 : [1, 2, 3]$.	.
.	$z_2 : [1, 2, 3]$	$x^3 + 2x^2 - 8x - 8$	3136 <i>x</i> ₁
.	$z_{1,2}$	$x^6 + 3x^5 - 8x^4 - 21x^3 + 6x^2 + 24x + 8$	Kummer
27-29	$z_1 : [1, 2, 3]$.	.
.	$z_3 : [1, 2, 3]$	$x^3 + 3x^2 - 18x - 27$	1764 <i>j</i> ₁
.	$z_{1,3} : [1, 2, 3]$	$x^6 + 4x^5 - 17x^4 - 52x^3 + 6x^2 + 72x + 27$	Kummer
9-14&21-26	$z_{1,2}$.	.
	$z_5 : [1, 2, 4, 5, 8, 10]$	$x^6 - x^5 - 6x^4 + 6x^3 + 8x^2 - 8x + 1$	Kummer

Table 3. The algebra for the character table of group $G_7 := (336, 118)$. In column 1 are the characters in question. Column 2 provides the powers of the entries z_i , $i = 1, 2, 3$ or 5. The z_i are $z_1 = 2 \cos(2\pi/7)$, $z_2 = 2z_1$, $z_3 = -6 \cos(\pi/7)$, $z_4 = \sqrt{2}$ and $z_5 = 2 \cos(2\pi/21)$. Column 3 explicits the polynomial $f(x)$ whose roots are the powers of a selected z_i . When $f(x)$ is an elliptic curve defined over the rationals the Cremona reference is in column 4. If $f(x)$ is a sextic polynomial it leads to a Kummer surface.

159 A summary of the elliptic and genus 2 hyperelliptic curves that can be defined from G_7 is in Table
160 3.

161 For instance, characters 4 to 6 as obtained from Magma [13] contains non constant entries with
162 $z_1, z_1\#2$ and $z_1\#3$. With the polynomial $f(x) = (x - z_1)(x - z_1\#2)(x - z_1\#3)$ one defines the elliptic
163 curve $y^2 = f(x)$ over the rationals whose conductor N and discriminant Δ are equal to 784 and whose
164 j -invariant equals 1792. It corresponds to the isogeny class of the curve 784i₁ in the Cremona table [12].

165 There are 12 characters containing entries with z_5 . We now show an important characteristics of
166 such characters. As an example, let us write the character number 9 as obtained from Magma [13]

$$\kappa_9 = [2, 2, -1, 2, 0, -1, z_1\#3, z_1\#2, z_1, 0, 0, z_1\#2, z_1\#3, z_1, z_5, z_5\#4, z_5\#8, z_5\#10, z_5\#2, z_5\#5, z_1\#2, z_1, z_1\#3, z_5\#8, z_5\#5, z_5\#2, z_5, z_5\#4, z_5\#10]$$

167 The hyperelliptic curve $\mathcal{C}_7 : y^2 = f(x)$ attached to the Kummer surface defined over the group
168 $G_7 := (336, 118)$ is

$$y^2 = f(x) = (x - k)(x - l)(x - m)(x - n)(y - o)(y - p), \quad (2)$$

169 with $k = 2 \cos(10\pi/21)$, $l = 2 \cos(4\pi/21)$, $m = 2 \cos(16\pi/21)$, $n = 2 \cos(2\pi/21)$ and $o =$
170 $-2 \cos(\pi/21)$ (as above) and $p = \cos(\pi/21) + \cos(8\pi/21) - \cos(6\pi/21)$. The sum of roots of the
171 sextic curve $f(x)$ equals 1.

172 The defining polynomial can be given an explicit expression over the rational field

$$f(x) = x^6 - x^5 - 6x^4 + 6x^3 + 8x^2 - 8x + 1,$$

173 leading to the Kummer surface

$$\begin{aligned} K3(x_1, x_2, x_3, x_4) = & 32x_1^4 - 24x_1^3x_2 + 96x_1^3x_3 - 4x_1^3x_4 + 24x_1^2x_2^2 \\ & - 196x_1^2x_2x_3 + 16x_1^2x_2x_4 + 240x_1^2x_3^2 - 32x_1^2x_3x_4 + 4x_1x_2^3 - 24x_1x_2^2x_3 \\ & - 12x_1x_2x_3x_4 + 12x_1x_3^3 + 24x_1x_3^2x_4 - 4x_1x_3x_4^2 - 4x_2^4 + 32x_2^3x_3 - 32x_2^2x_3^2 \\ & + x_2^2x_4^2 - 24x_2x_3^3 + 2x_2x_3^2x_4 + 25x_3^4. \end{aligned}$$

174 A section at constant x_4 of this Kummer surface is given in Fig. 2b using the MathMod software
175 [14].

176 The desingularisation of the Kummer surface is obtained by restricting the product in the
177 polynomial $f(x)$ to the five first factors. It is found that the corresponding Jacobian of \mathcal{C}_7 has 16 = 6 + 10
178 points as follows

179 * the 6 points bounded by the modulus 1:

180 $Id := (1, 0, 0)$, $K := (x - k, 0, 1)$, $L := (x - l, 0, 1)$, $N := (x - n, 0, 1)$, $M := (x - m, 0, 1)$ and
181 $O := (x - o, 0, 1)$.

182 * the 10 points of modulus > 1: $a_1 := K + L$, $a_2 := K + M$, $a_3 := K + N$, $a_4 := K + O$, $a_5 := L + N$,
183 $a_6 := K + L + M$, $a_7 := K + L + N$, $a_8 := K + L + O$, $a_9 := 2K + L + M$ and $a_{10} := 2K + L + O$.

184 More explicitly, for instance, $K + L = (x^2 - (k + l)x + 2 \cos(2\pi/7), 0, 2)$.

185 The 16 points organize as a commutative group isomorphic to the maximally abelian group \mathbb{Z}_2^4 as
186 shown in table 2 with the entries

$$\begin{aligned}
 A : & \begin{bmatrix} Id & K & L & a_1 \\ K & Id & a_1 & L \\ L & a_1 & Id & K \\ a_1 & L & K & Id \end{bmatrix}, & B : & \begin{bmatrix} N & a_3 & a_5 & a_7 \\ a_3 & N & a_7 & a_5 \\ a_5 & a_7 & N & a_3 \\ a_7 & a_5 & a_3 & N \end{bmatrix} \\
 C : & \begin{bmatrix} M & a_2 & a_9 & a_6 \\ a_2 & M & a_6 & a_9 \\ a_9 & a_6 & M & a_2 \\ a_6 & a_9 & a_2 & M \end{bmatrix}, & D : & \begin{bmatrix} a_8 & a_{10} & a_4 & O \\ a_{10} & a_8 & O & a_4 \\ a_4 & O & a_8 & a_{10} \\ O & a_4 & a_{10} & a_8 \end{bmatrix}.
 \end{aligned}$$

187 There are 12 points in the Jacobian of \mathcal{C}_7 bounded by the modulus 1: the 6 points in the Jacobian
 188 of \mathcal{C} as above and 6 extra points, $(1 : 1 : 0)$ (an extra point at infinity), $(0 : 1 : 1)$, $(0 : -1 : 1)$, $(1 : 1 : 1)$,
 189 $(1 : -1 : 1)$ (4 rational points) and the point $P := (x - p, 0, 1)$.

190 One finds 70 points bounded by the modulus 2 or 3, 694 points bounded by the modulus 4 and so
 191 on.

192 3. The genetic code revisited

193 Our theory of the genetic code takes its inspiration in the symmetries observed in the DNA
 194 double helix and the biological steps leading to the conversion of transfer RNA (tRNA) into the
 195 amino acids that code for proteins. While 5-fold symmetry is inherent to the DNA double helix, being
 196 present in all its constituents, as shown in Fig. 1a, the way to transcription into proteins needs an
 197 extra step in the spliceosome. The spliceosome is found within the nucleus of eukaryotic cells. Its
 198 role is to remove introns from the primary form of messenger RNA (mRNA) leaving the exons to
 199 be processed afterwards. This cutting process is called splicing. There is a heptamer ring, called the
 200 Lsm 1-7 complex, displaying a 7-fold symmetry in its protein constituents, as shown in Fig. 1c [7].
 201 Accounting for this observation, it is tempting to generalize our theory of the genetic code based on the
 202 22 irreducible characters of the group $G_5 := (240, 105) \cong \mathbb{Z}_5 \rtimes 2O$, displaying the 5-fold symmetry, to
 203 the 29 irreducible characters of the group $G_7 := (336, 118) \cong \mathbb{Z}_7 \rtimes 2O$, displaying the 7-fold symmetry.
 204 The group G_6 is not an appropriate candidate for modeling the degeneracies of amino acids in the
 205 genetic code since none irreducible character of G_6 is informationally complete, as shown in Table 1.

206 In Table 5 of the appendix, we reproduce the structure of the character table of the group G_5
 207 and the assignments of its conjugacy classes to the proteinogenic amino acids as given in Ref. [1].
 208 One drawback of the model is that there are only 2 sextets in the table while 3 of them are needed to
 209 fit the 3 sextets of the genetic code. In Table 4, this problem is solved since there are precisely three
 210 slots of degeneracy 6 in the character table of G_7 . Table 4 shows entries proportional to the cosines
 211 of angles involved in the characters as $z_1 = 2 \cos(2\pi/7)$, $z_2 = 2z_1$, $z_3 = -6 \cos(\pi/7)$, $z_4 = \sqrt{2}$ and
 212 $z_5 = 2 \cos(2\pi/21)$. Let us first concentrate on the 11 classes of degeneracy 2 of the group G . The
 213 character table contains the angle $2\pi/8$ through the 2 entries with $z_4 = 2 \cos(2\pi/8) = \sqrt{2}$ as well as
 214 the angles $2\pi/7$ and $2\pi/21$ through the entries with z_1 and $z_{1,5}$, respectively. We choose not to assign
 215 amino acids to the 2 conjugacy classes with degeneracy 2 and $2\pi/8$ angle. The entries containing z_5
 216 correspond to the hyperelliptic curve $y^2 = f(x)$ in (2) and the related Kummer surface. Then, there
 217 are two conjugacy classes with degeneracy 1 (ignoring the class with a trivial character) and 3, as
 218 expected. There are 3 classes with degeneracy 6 with entries containing z_3 and thus the angle $2\pi/7$, as
 219 we would expect. Finally, there are 10 slots for quartets but only 5 slots with entries containing the
 220 entry z_5 related to the Kummer surface. The first 4 slots are assigned to the 4 (degeneracy 4) amino
 221 acids and a slot is left empty. This leaves the freedom to assign this slot to the 21st proteinogenic acid
 222 Sec and the 22nd amino acid Pyl (compare to [1] or Table 5).

223 Now comes a question. Is the Kummer surface an attribute of RNA packings or is the proposed
 224 theory just another musing about the biological reality? We are not aware of any experiment featuring
 225 the Kummer surface in the biological realm. The physical link between messenger RNA (mRNA) and

(336,118) $\mathbb{Z}_7 \times (\mathbb{Z}_2.S_4)$ $\cong \mathbb{Z}_7 \times 2O$	dimension d-dit, d=29 amino acid	1 29 .	1 785 Met	1 d^2 Trp	2 d^2 Cys	2 d^2 Phe	2 d^2 Tyr	2 d^2 .	2 d^2 .	2 d^2 His	2 d^2 Gln
	order char polar req.	1 Cte .	2 Cte 5.3	3 Cte 5.2	4 z_1 4.8	4 z_1 5.0	6 z_1 5.4	7 z_4 .	7 z_4 .	7 $z_{1,5}$ 8.4	8 $z_{1,5}$ 8.6
(336,118)	dimension d-dit, d=29 amino acid	2 d^2 Asn	2 d^2 Lys	2 d^2 Glu	2 d^2 Asp	3 d^2 Ile	3 d^2 Stop	4 d^2 .	4 d^2 .	4 d^2 .	4 d^2 .
	order char polar req.	14 $z_{1,5}$ 10.0	14 $z_{1,5}$ 10.1	14 $z_{1,5}$ 12.5	21 $z_{1,5}$ 13.0	21 Cte 10	21 Cte 15	21 Cte .	21 $z_{1,2}$.	21 $z_{1,2}$.	21 $z_{1,2}$.
(336,118)	dimension d-dit, d=29 amino acid	4 d^2 Val	4 d^2 Pro	4 d^2 Thr	4 d^2 Ala	4 d^2 Gly	4 d^2 .	6 d^2 Leu	6 d^2 Ser	6 d^2 Arg	
	order char polar req.	28 $z_{2,5}$ 5.6	28 $z_{2,5}$ 6.6	28 $z_{2,5}$ 6.6	42 $z_{2,5}$ 7.0	42 $z_{2,5}$ 7.9	42 $z_{2,5}$.	42 $z_{1,3}$ 4.9	42 $z_{1,3}$ 7.5	42 $z_{1,3}$ 9.1	

Table 4. For the group $G_7 := (336, 118) \cong \mathbb{Z}_7 \times 2O$, the table provides the dimension of the representation, the rank of the Gram matrix obtained under the action of the 29-dimensional Pauli group, the order of a group element in the class, the angles involved in the character and a good assignment to an amino acid according to its polar requirement value. Bold characters are for faithful representations. All characters are informationally complete except for the trivial character and the one assigned to 'Met'. The entries involved in the characters are $z_1 = 2 \cos(2\pi/7)$, $z_2 = 2z_1$, $z_3 = -6 \cos(\pi/7)$, $z_4 = \sqrt{2}$ and $z_5 = 2 \cos(2\pi/21)$ featuring the angles $2\pi/8$ (in z_4), $2\pi/7$ and $2\pi/21$.

226 the amino acid sequence of proteins is a transfer RNA (tRNA). Corresponding to the three bases of
 227 an mRNA codon is an anticodon. Each tRNA has a distinct anticodon triplet sequence that can form
 228 three complementary base pairs to one or more codons for an amino acid. Some anticodons pair with
 229 more than one codon due to so-called wobble base pairing [15]-[18]. Considering the secondary and
 230 tertiary structure of tRNA, as well as the fact that the third position in the codon is not strictly red by
 231 the anticodon according to Watson-Crick pairing rules, Crick hypothesized that codon translation into
 232 a proteins is mainly due to the first two positions of the codon [15]. There are 16 groups of codons
 233 specified by the first two codonic positions and the level of degeneracy can be derminded by them
 234 according to Lagerkvist's rules [16,17]. Our bet is that the 16 groups of codons correspond to the 16
 235 singularities (double points) of the Kummer surface.

236 In the next section, we discuss the relevance of the Kummer surface in the context of 4-dimensional
 237 (space-time) quantum gravity.

238 4. Kummer surface and quantum gravity

239 The Kummer surface first made its appearance in the Fresnel wave equation for light in a biaxial
 240 crystal [19,20]. The four singularities corresponding to the two shells in the Fresnel surface for a biaxial
 241 crystal lead to internal conical refraction as predicted by Hamilton in 1832. It is also known that, for a
 242 magnetoelectric biaxial crystal, the Fresnel surface may display 16 real singular points, the maximal
 243 number permitted for a linear material whose dispersion relation is quartic in the frequency and/or
 244 wave number [20]. Although Kummer surface is relevant to electromagnetism, Ref. [21] discusses how
 245 it may also rely on gravity.

246 A theory of quantum gravity needs to conciliate our view of space-time as described by the
 247 general relativity and our view of particles and fields as described by quantum mechanics or quantum
 248 field theory. How is the Kummer surface related to attempts of formulating a theory of quantum
 249 gravity?

If one follows the historical perspective, our derivation of the Kummer surface in Sec. 2 relies on the work of Felix Klein in 1870 [19,22]. He introduces a quadratic line complex as the intersection $X = \text{Gr}(2,4) \cap W$ of the Grassmann quadric $\text{Gr}(2,4)$ in the five-dimensional Plücker space with another quadratic hypersurface W . The set of lines in X is parametrized by the Jacobian $\text{Jac}(C)$ of a Riemann surface of genus 2 ramified along 6 points corresponding to 6 singular quadrics. See [23] for the relation to string dualities.

Nowadays, in the classification by algebraic geometry, the Kummer surface is an example of a K_3 surface built from the quotient of an abelian variety A by the action from a point a to its opposite $-a$, resulting in 16 singularities [24,25]. The minimal resolution is the Kummer surface. There are many constructions of a K_3 surface Y and it is known that all of them are diffeomorphic to each other. A K_3 surface is a compact connected complex manifold of dimension 2 with trivial first Chern class $c_1(Y) = 0$ so that the second Chern class (which corresponds to the topological Euler characteristic) is $c_2(Y) = 24$. Another important topological invariant of topological spaces is that of a Betti number b_k . Roughly, b_0 is the number of connected components, b_1 is the number of one-dimensional ‘holes’, b_2 is the number of two-dimensional ‘voids’, and so on. For a K_3 surface, one has $b_0=b_4=1$, $b_1=b_3=0$ and $b_2=22$. This defines Y as the unique unimodular even quadratic lattice of signature $(3,19)$ isomorphic to $E_8(-1)^{\oplus 2} \oplus U^{\oplus 3}$, where U the integral hyperbolic plane and E_8 is the well known E_8 lattice. It is also known that the elliptic genus of a K_3 surface has a decomposition in terms of the dimensions of irreducible representations of the largest Mathieu group M_{24} [26], a concept named ‘umbral moonshine’. See also [27] for another view of the latter topic.

In the forefront of differential geometry, there is a connection of K_3 surfaces to quantum gravity in the concept of a Kähler manifold (with a Kähler metric). Such a manifold possesses a complex structure, a Riemannian structure and a symplectic structure. A K_3 surface admits a Kähler ‘Ricci-flat metric’ although it is not known how to write it in an explicit way. It is worthwhile to mention that a K_3 surface appears in string theory with the concept of ‘string duality’—how distinct string theories are related—, see Ref. [23,28]. Another work relating quantum gravity and K_3 surfaces is in Ref. [29]-[31].

5. Discussion

Since the Kummer surface appears in our models of DNA/RNA packings of some protein complexes such as the hexamer and pentamer rings (the LSMs, MCMs and other biological complexes not given here) one can ask the question whether quantum gravity is relevant in such biological realms. It is a challenging question that we are not able to solve. Mathematics offers clues for models of nature. Biology is not an unified field as is quantum physics of elementary particles or the general relativity for the universe at large scales. We offered relationships between the n -fold symmetries ($n = 5, 6$ and 7) found in DNA and some proteins and the mathematics of Kummer surfaces. It is time to quote earlier work devoted to the possible relation between the microtubules of cytoskeleton and the field of quantum consciousness, e.g. [32]. The 13-fold symmetry is found in tubulin complexes [33]. Using the same approach than the one for DNA and hexamer/pentamer complexes, we can associate a finite group $G_{13} := (624, 134) \cong \mathbb{Z}_{13} \times 2O$ to such a 13-fold symmetric complex. Such a group possesses 50 conjugacy classes and the dimensions of representations are 1, to 2, 3, 4 and 6 as expected for this series of groups with factors \mathbb{Z}_n and $2O$ in the semidirect product. It is found that a Kummer surface may be derived from some characters of G_{13} , as expected.

To conclude, one can observe a mathematical analogy between the way DNA/RNA organize and some theories of quantum cosmology based on string dualities. Lessons from one field may lead to progress in the other field. Should we talk about a new paradigm of ‘biologic quantum cosmology’ and revisit the philosophical foundations of quantum theory? A few papers are already written in this direction [34,35] and [36].

Author Contributions: Conceptualization, M.P., F.F. and K.I.; methodology, D.C., M.P. and R.A.; software, M.P.; validation, D.C., R.A., F.F. and M.A.; formal analysis, M.P. and M.A.; investigation, D.C., M.P., F.F. and M.A.; writing—original draft preparation, M.P.; writing—review and editing, M.P.; visualization, D.C., F.F. and R.A.;

309 supervision, M.P. and K.I.; project administration, K.I.; funding acquisition, K.I. All authors have read and agreed
300 to the published version of the manuscript.

301 **Funding:** Funding was obtained from Quantum Gravity Research in Los Angeles, CA

302 **Conflicts of Interest:** The authors declare no conflict of interest.

303 References

- 304 1. M. Planat, R. Aschheim, M. M. Amaral, F. Fang and K. Irwin, Complete quantum information in the DNA
305 genetic code, *Symmetry* **12** 1993 (2020).
- 306 2. M. Planat and Z. Gedik, Magic informationally complete POVMs with permutations, *R. Soc. open sci.* **4**
307 170387 (2017).
- 308 3. M. Planat, R. Aschheim, M. M. Amaral and K. Irwin, Informationally complete characters for quark and
309 lepton mixings, *Symmetry* **12** 1000 (2020).
- 310 4. C. Sauter, J. Basquin and D. Suck, Sm-Like proteins in eubacteria: the crystal structure of the Hfq protein
311 from Escherichia Coli, *Nucleic Acids* **31** 4091 (2003), <https://www.rcsb.org/structure/1HK9>.
- 312 5. W. C.L. Lührmann, Spliceosome, structure and function, *Cold Spring Harbor Perspectives in Biology* **3** a003707
313 (2011).
- 314 6. C. Kambach, S. Walke, R. Young, J. M. Avis, E. de la Fortelle, V. A. Raker, R. Lührmann, J. Li and K. Nagai,
315 Crystal structures of two Sm protein complexes and their implications for the assembly of the spliceosomal
316 snRNPs, *Cell* **96** 375–87 (1999).
- 317 7. L. Zhou, Y. Zhou, J. Hang, R. Wan, G. Lu, C. Yan and Y. Shi, Crystal structure and biochemical analysis of the
318 heptameric Lsm1-7 complex, *Cell Research* **24** 497–500 (2014).
- 319 8. Z. Kelman, J. Finkelstein and M. O'Donnel, Why have six-fold symmetry? *Current Biology* **5** 1239–42 (1995).
- 320 9. Y. Zhai, E. Cheng, H. Wu, N. Li, P. Y. Yung, N. Gao and B. K. Tye, Open-ringed structure of the Cdt1–Mcm2–7
321 complex as a precursor of the MCM double hexamer, *Nature Structural & Molecular Biology.* **24** 300–308 (2017).
- 322 10. M. Planat, R. Aschheim, M. M. Amaral and K. Irwin, Group geometrical axioms for magic states of quantum
323 computing, *Mathematics* **7** 948 (2019).
- 324 11. R. W.H.T. Hudson, Kummer's quartic surface, Cambridge Univ. Press 1990, First published 1905.
- 325 12. LMFDB-The Lf unctions and modular forms database. <https://www.lmfdb.org/> accessed on 1 June 2020.
- 326 13. Bosma, W.; Cannon, J. J.; Fieker, C. ; Steel, A. (eds). *Handbook of Magma functions*, Edition 2.23 (2017), 5914pp
327 (accessed on 1 January 2019).
- 328 14. <https://sourceforge.net/projects/mathmod/> (accessed on 1 December 2020).
- 329 15. F. HC Crick, Codon-anticodon pairing, the wobble hypothesis, *J. Mol. Biol.* **19** 548–555 (1966).
- 330 16. U. Lagerkvist, "Two out of tree": an alternative method for codon reading, *Proc. Natl. Acad. Sci.* **75** 1759–1762
331 (1978).
- 332 17. J. Lehmann and A. Lichbaber, Degeneracy of the genetic code and stability of the base pair at the second
333 position of the anticodon, *RNA* **14** 1264–1269 (2008).
- 334 18. D. L. Gonzalez, S. Giannerini and M. Rosa, On the origin of degeneracy in the genetic code, *Interface Focus* **9**
335 20190038(2019).
- 336 19. I. Dolgachev, Kummer surfaces: 200 years of study, *Notices of the AMS* **67** 1527–33 (2020).
337 Preprint 1910.07650 [math.AG].
- 338 20. A. Favaro and F. W. Hehl, Light propagation in local and linear media: Fresnel-Kummer wave surfaces with
339 16 singular points, *Phys. Rev. A* **93** 013844 (2016).
- 340 21. P. Baekler, A. Favaro, Y. Itin and F. W. Hehl, The Kummer tensor density in electrodynamics and in gravity,
341 *Ann. Phys.* **349** 297–324 (2014).
- 342 22. C. Jessop, *A treatise of the line complex* (Cambridge University Press, 1903). [reprinted by Chelsea Pibl. Co.,
343 N.Y., 1969).
- 344 23. A. Clingher, A. Malmendier and T. Shaska, Six line confihurations and string dualities, *Commun. Math. Phys.*
345 **371** 159–196 (2019).
- 346 24. R. E. Gompf and A. I. Stipsicz, *4-manifolds and Kirby calculus*, Graduate Studies in Mathematics, Vol. 20
347 (American Mathematical Society, Providence, Rhode Island, 1999).
- 348 25. A. Scorpián, *The wild world of 4-manifolds* (American Mathematical Society, Providence, Rhode Island, 2011).

- 349 26. T. Eguchi, H. Ooguri and Y. Tachikawara, Notes on the K_3 surface and the Mathieu group M_{24} , *Exp. Math.*
 350 **20** 91–96 (2011).
- 351 27. A. Marrani, M. Rios and D. Chester, Monstruous M -theory, Preprint Arxiv 2008.06742v1 [hep-th].
- 352 28. P. S. Aspinwall, K_3 surfaces and string duality, in C. Efthimiou and B. Greene, editors, “Fields, Strings and
 353 Duality, TASI 1996”, pp 421–540, World Scientific, 1997 (Preprint hep-th/9611137).
- 354 29. T. Asselmeyer-Maluga, Smooth Quantum Gravity: Exotic Smoothness and Quantum Gravity. In *At
 355 the Frontiers of Spacetime: Scalar-Tensor Theory, Bell’s Inequality, Mach’s Principle, Exotic Smoothness* (T.
 356 Asselmeyer-Maluga, Ed.; Springer: Basel, Switzerland, 2016).
- 357 30. T. Asselmeyer-Maluga, Braids, 3-manifolds, elementary particles, number theory and symmetry in particle
 358 physics, *Symmetry* **10** 1297 (2019).
- 359 31. M. Planat, R. Aschheim, M. M. Amaral and K. Irwin, Quantum computation and measurements from an
 360 exotic space-time R^4 , *Symmetry* **12** 736 (2020).
- 361 32. S. Hameroff and R. Penrose, Consciousness in the universe, a review of the ‘Orch OR’ theory, *Phys. of Life
 362 Rev.* **11** 39–78 (2014).
- 363 33. J. M. Kollmann, J. K. Polka, A. Zelter, T. N. Davis and D. Agard, Microtubule nucleating γ TuSC assembles
 364 structures with 13-fold microtubule-like symmetry, *Nature* **466** 879-882 (2012).
- 365 34. Yi-Fang Chang, Calabi-Yau manifolds in biology and biological string-brane theory, **4** 465–474 (2015).
- 366 35. R. Pincak, K. Kanjamapornkul and E. Bartos, A theoretical investigation of the predictability of genetic
 367 patterns, *Chem. Phys.* **535** 110764 (2020).
- 368 36. K. Irwin, M. Amaral and D. Chester, The Self-Simulation hypothesis interpretation of quantum mechanics,
 369 *Entropy* **22** 247 (2020).

370 6. Appendix

371 The table below was found in our paper [1]. An introduction to the DNA genetic code and the
 372 mention to some mathematical theories proposed before is discussed in this paper and not duplicated
 373 here.

$(240,105)$ $\mathbb{Z}_5 \times (\mathbb{Z}_2.S_4)$ $\cong \mathbb{Z}_5 \times 2O$	dimension d-dit, d=22 amino acid	1 d^2 Met	1 d^2 Trp	2 d^2 Cys	2 d^2 Phe	2 d^2 Tyr	2 d^2 His	2 d^2 Gln	2 d^2 Asn	2 d^2 Lys	2 d^2 Glu	2 d^2 Asp
	order	1	2	3	4	4	5	5	6	8	8	10
	char	Cte	Cte	Cte	z_1	z_1	z_4	z_4	$z_{1,5}$	$z_{1,5}$	$z_{1,5}$	$z_{1,5}$
	polar req.	5.3	5.2	4.8	5.0	5.4	8.4	8.6	10.0	10.1	12.5	13.0
$(240,105)$	dimension d-dit, d=22 amino acid	3 d^2 Ile	3 d^2 Stop	4 d^2 Leu,Pyl,Sec	4 d^2 Leu	4 d^2 Val	4 d^2 Pro	4 d^2 Thr	4 d^2 Ala	4 d^2 Gly	6 d^2 Ser	6 d^2 Arg
	order	10	15	15	15	15	20	20	30	30	30	30
	char	Cte	Cte	Cte	$z_{1,2}$	$z_{1,2}$	$z_{2,5}$	$z_{2,5}$	$z_{2,5}$	$z_{2,5}$	$z_{1,3}$	$z_{1,3}$
	polar req.	4.9			4.9	5.6	6.6	6.6	7.0	7.9	7.5	9.1

Table 5. For the group $G_5 := (240,105) \cong \mathbb{Z}_5 \times 2O$, the table provides the dimension of the representation, the rank of the Gram matrix obtained under the action of the 22 -dimensional Pauli group, the order of a group element in the class, the entries involved in the character and a good assignment to an amino acid according to its polar requirement value. Bold characters are for faithful representations. There is an ‘exception’ for the assignment of the sextet ‘Leu’ that is assumed to occupy two 4-dimensional slots. All characters are informationally complete except for the ones assigned to ‘Stop’, ‘Leu’, ‘Pyl’ and ‘Sec’. The notation in the entries is as follows: $z_1 = -(\sqrt{5} + 1)/2$, $z_2 = \sqrt{5} - 1$, $z_3 = 3(1 + \sqrt{5})/2$, $z_4 = \sqrt{2}$, $z_5 = -2 \cos(\pi/15)$, compare [1, Table 7].